

Synthesis and Characterization of Lithium Iron Phosphate Carbon Composite (LFP/C) using Magnetite Sand Fe_3O_4

Zuffa Anisa,^{*1} Mochammad Zainuri²

¹Chemistry Department, Faculty of Science and Engineering, University of Bojonegoro

²Physics Department, Faculty of Mathematic and Sciences, Institute Technology of Sepuluh Nopember

*Corresponding email : zuffa.anisa@gmail.com

Received 22 November 2019; Accepted 15 April 2020

ABSTRACT

Lithium Ferro Phosphate Carbon Composite (LFP/C) had been synthesized using solid-state reaction method. Magnetite sand Fe_3O_4 was used as Fe- source in LFP/C synthesized. Calcination temperature of the sample performed at 400, 500, and 600°C. The phase and composition of samples determined by Rietveld analysis of X-ray diffraction (XRD) pattern. The dominant identified phase at 400°C was diphosphate LiFeP_2O_7 , and the others phases were nasicon $\text{Li}_3\text{Fe}_2(\text{PO}_4)_3$ and hematite Fe_2O_3 . As the temperature getting higher the diphosphate phase LiFeP_2O_7 transform to nasicon $\text{Li}_3\text{Fe}_2(\text{PO}_4)_3$. The chemical bonds, lattice vibration and other structural features of the sample were investigated using FTIR spectroscopy in range of 1400 – 400 cm^{-1} . Specific vibration modes in LFP-1 to LFP-3 for each bonding were shown by the high intense in certain wavenumber.

Key word: LFP/C, Magnetite, Nasicon, Diphosphate, Phase

INTRODUCTION

The demand for rechargeable batteries, lithium-ion batteries has increased significantly. Unfortunately several lithium batteries such as LiCoO_2 , LiNiO_2 are toxic and not environmentally benign [1]. Another efforts has paid attention by using Fe-based material as an alternative replacement for the active materials of Lithium Ferro Phosphate (LFP) in lithium ions batteries. Recently, the LFP has also attracted manufacturer interest because it has a lot of advantages like charging capacity and many others. The theoretical charging capacity of LFP is 170 mAh/g [2]. And also, it has a high value of capacity than the other cathode materials such as LiMn_2O_4 with 117 mAh/g charging capacity. Moreover, the LFP is environmentally more benign material than the other cathode materials. For example LiCoO_2 , indicates toxicity issue and also costly in preparation. Conversely, the LFP based materials also has a good cycle stability, and excellent thermal stability. These advantages, coupled with abundantly source of iron for the LFP synthesis become a promising and reasonable concern for production. However, the LFP based material has a low electrical conductivity. This paper applies citric acid as a carbon source was to be added to make a Lithium Iron Phosphate Carbon composite (LFP/C) for overcoming of the drawback [3].

Research using natural iron sand composed of Fe_3O_4 , can be used as iron sources to form LFP/C precursor are still a wide apart. Some divalent and trivalent Fe-sources such as $\text{FeC}_2\text{O}_4 \cdot 2\text{H}_2\text{O}$, $\text{Fe}(\text{CH}_3\text{COO})_2$, FeSO_4 , and $\text{Fe}(\text{NO}_3)_3$ had been practiced as well [4]. However, these materials are still very expensive and even some of them are toxics.

The journal homepage www.jpacr.ub.ac.id

p-ISSN : 2302 – 4690 | e-ISSN : 2541 – 0733

Based on the preliminary study indicated that the natural iron sand from Tanah Laut Kalimantan, Indonesia, contained 98% of Fe. It was analyzed using x-ray fluorescence (XRF) spectrometer. Further analysis using x-ray diffraction (XRD) spectrometer showed the natural iron sand phase was identified as magnetite Fe_3O_4 . The Fe_3O_4 is composed of $\text{FeO}\cdot\text{Fe}_2\text{O}_3$ which have trivalent Fe^{3+} in Fe_2O_3 and divalent Fe^{2+} ion in FeO . This paper reports the work result of applying of this natural iron sand from this specific location for LFP/C precursor. Several papers have reported similar concerns, due to the electrochemical performance of Fe_3O_4 and also the low-cost production potency. However no work have been reported in manufacturing using of the local Indonesian resources. Many methods have been used to make LFP/C such as coprecipitation, solvothermal, hydrothermal, solid-liquid, and freeze granulation [5], but some of them are rather complicated. In this study, LFP/C was synthesized by a simple methodology, and implementing of the solid state synthesis strategy using high energy ball milling process [6,7].

EXPERIMENT

Chemicals and Instrumentation

Materials used for this research were lithium carbonate Li_2CO_3 (Sigma-Aldrich), diammonium hydrogen phosphate $(\text{NH}_4)_2\text{HPO}_4$ (Sigma-Aldrich) with purity >98%, citric acid $\text{C}_8\text{H}_8\text{O}_7\cdot\text{H}_2\text{O}$, and natural iron sand with 98% Fe element content.

The instruments used for this study are oven, furnace, differential scanning calorimetric-thermal gravimetric analysis (DSC-TGA) (Mettler Toledo Star SW 10.0, thermal analysis from room temperature to 1400 °C and sample weight 15.2 mg), x-ray diffraction (XRD) spectrometer (Siemens D-501, Ni filter and graphite monochromator, x-ray source from Cu K α radiation λ 1.5406 Å, with scanning angle from 15° to 65°) to identify the phase of LFP/C, and the FTIR spectrophotometer (recorded in Shimadzu 8400S).

Synthesis of Precursor

LFP/C compounds were prepared by high energy ball milling method [8]. The materials being used are Li_2CO_3 , $(\text{NH}_4)_2\text{HPO}_4$, and Fe_3O_4 with 3:6:2 of mole ratio. A 5.0% weight citric acid as carbon sources was added to these materials to enhance the electron conductivity and to avoid oxidation of Fe ion. Then, 5.0 mL of alcohol was poured into a milling jar and milled together in 300 rpm rotation speed, for 3 hours. The resulted precursor was dried at 100°C (LFP-0) in oven. Then, similar procedure was applied and calcination was undergone in different temperature, i.e. 400°C (LFP-1), 500°C (LFP-2), and 600°C (LFP-3).

Characterization

The thermal properties of the sample was investigated using DSC-TGA for determine the variation temperature will be given to the sample. The calcination temperatures were varied in the range of (400-700 °C) to observe the formed phases of Lithium Ferro Phosphate Carbon composite (LFP/C) [9]. The sample before getting heat treatment named LFP-0, while the samples had been calcinated in 400, 500, and 600 °C named LFP-1, LFP-2, and LFP-3 respectively. XRD was adopted to identify crystalline phases on the samples. Chemical bonds, structural properties, and lattice dynamics was examined by Fourier Transformed Infrared Spectroscopy (FTIR). The crystalline phases and its composition in the XRD pattern were analyzed using Search Match software qualitatively and Rietica quantitatively.

RESULT AND DISCUSSION

DSC-TGA Analysis

The thermal properties of LFP/C were analyzed using DSC-TGA at room temperature until 1300°C. A large negative gradient at 100 to 300°C range temperature indicates a significant mass reduction in sample weight. The heat flow diagram in figure 1 shows that there is a thermal phenomenon at 400°C until 700°C. This indicates, that within this temperatures, a phases transformation undergoes. It is showed by thermal uprising decline the mass of sample. At temperature 200-300 °C, a weight-mass loss is sharply observed. However, in temperature above 300°C, there is no significant mass reduction observed. Within this temperature range, the implemented heat can not reduce the the mass sample farther. However, it is predicted that, the heat radiated the sample is absorbed for a phase transformation. In this temperature, the phase of Lithium Ferro Phosphate LFP is formed. Phases transformation from the initial composition for Li_2CO_3 , $(\text{NH}_4)_2\text{HPO}_4$, and magnetite Fe_3O_4 , to other phases, such as diphosphate LiFeP_2O_7 , nasicon $\text{Li}_3\text{Fe}_2(\text{PO}_4)_3$ and hematite.

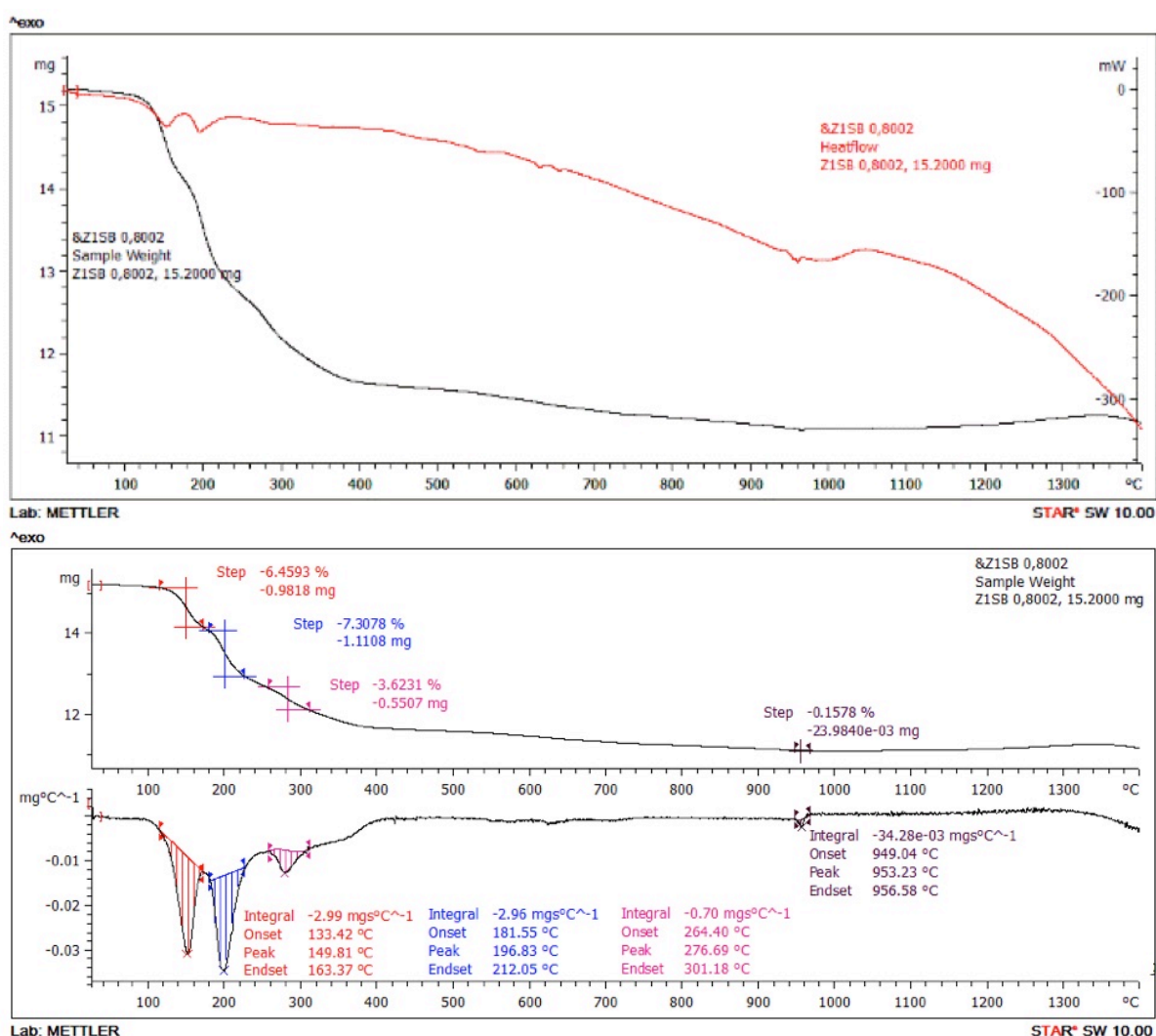


Figure 1. The result from DSC-TGA analysis of the sample

The detailed of mass loss of LFP/C from DTA-TGA analysis indicate the physical properties of this material. The stepwise loss occur in peak of 149.81 °C and 196.83 °C, and 276.69 °C. The mass loss recorded is 2.99, 2.96, and 0.70 mg/°C, respectively. It is predicted the decomposed of volatile compounds, such as water, alcoholic matter and ammonia. Furthermore, the rest of the temperature shows a steady line and is predicted that the compounds with a stable composition is formed.

XRD Analysis

Figure 2 is showed the XRD diffractogram of the samples lithium iron phosphahate/carbon composite (LFP/C) before and after calcination process. Calcination at 100 °C (LFP-0), 400 °C (LFP-1), 500 °C (LFP-2), and 600 °C (LFP-3). In overall, similar diffraction pattern is observed for LFP-1, LFP-2, and LFP-3. These similarity can also indicate similar composition and crystallinity of the LFP/C composite synthesized.

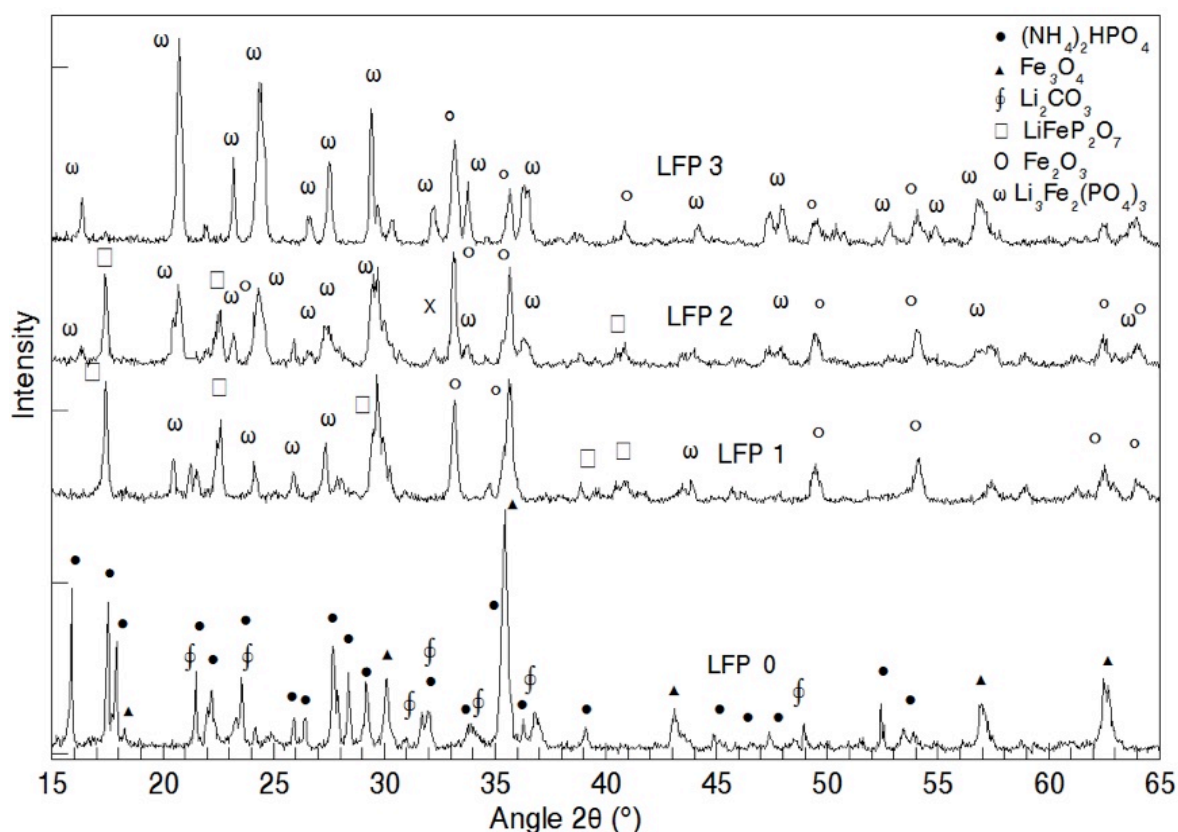


Figure 2. The XRD diffractogram of lithium iron phosphate/carbon (LFP/C) composite

Phase compositions of LFP-0 are 75.4: 16.9: 7.7 % weight comparison for $(\text{NH}_4)_2\text{HPO}_4$: Fe_3O_4 : Li_2CO_3 respectively. The formed phases at 400, 500, 600°C temperature are trigonal Fe_2O_3 , monoclinic LiFeP_2O_7 and $\text{Li}_3\text{Fe}_2(\text{PO}_4)_3$ [10], with the composition are summarized in Table 1. Calcination process at higher temperature give different LFP/C composite phase. The magnetite Fe_3O_4 is transformed become hematite Fe_2O_3 . The major phase was formed at 400°C (LFP-1) calcination is diphosphate LiFeP_2O_7 . Meanwhile, at higher temperature calcination, 500°C, the diphosphate phase of LiFeP_2O_7 is converted gradually, and turn it into nasicon $\text{Li}_3\text{Fe}_2(\text{PO}_4)_3$. Lastly, at the highest temperature

calcination, 600°C (LFP-3), the dominant phases formed are nasicon $\text{Li}_3\text{Fe}_2(\text{PO}_4)_3$ in 85.72%, in the absence of diphosphate LiFeP_2O_7 is observed.

Furthermore, it is also observed that increasing calcination temperature indicate crystal agglomeration undergone. The diphosphate form, LiFeP_2O_7 is predicted become triphosphate, $\text{LiFe}(\text{PO}_4)_3$ form. And also, the hematite Fe_2O_3 composition is gradually decreased and turn in trace. Previously, the presence of this kind impurity deteriorated the battery performance, such as cyclability, charge-discharge capacity, and conductivity [11]. Calcination at 600°C give the highest content of LFP and a very low of impurities.

Table 1. %-Weight phase composition of LFP/C after calcination

Sample	Diphosphate (LiFeP_2O_7) (%)	Nasicon ($\text{Li}_3\text{Fe}_2(\text{PO}_4)_3$) (%)	Hematite (Fe_2O_3) (%)
LFP-1	58.28	12.06	29.66
LFP-2	32.57	47.89	19.54
LFP-3	-	85.72	14.28

FTIR Analysis

Lattice dynamics of lithium iron phosphate-based materials composite in carbon (LFP-1, LFP-2, and LFP-3) are studied by using FTIR spectrophotometric. The presence of functional group of these materials in the surface are recorded as the vibrational of each group due to irradiated by photon in infra red wavelength. Absorbance values (in absorption unit) is correlated to the energy absorbed by the specific functional group composed in LFP/C composite.

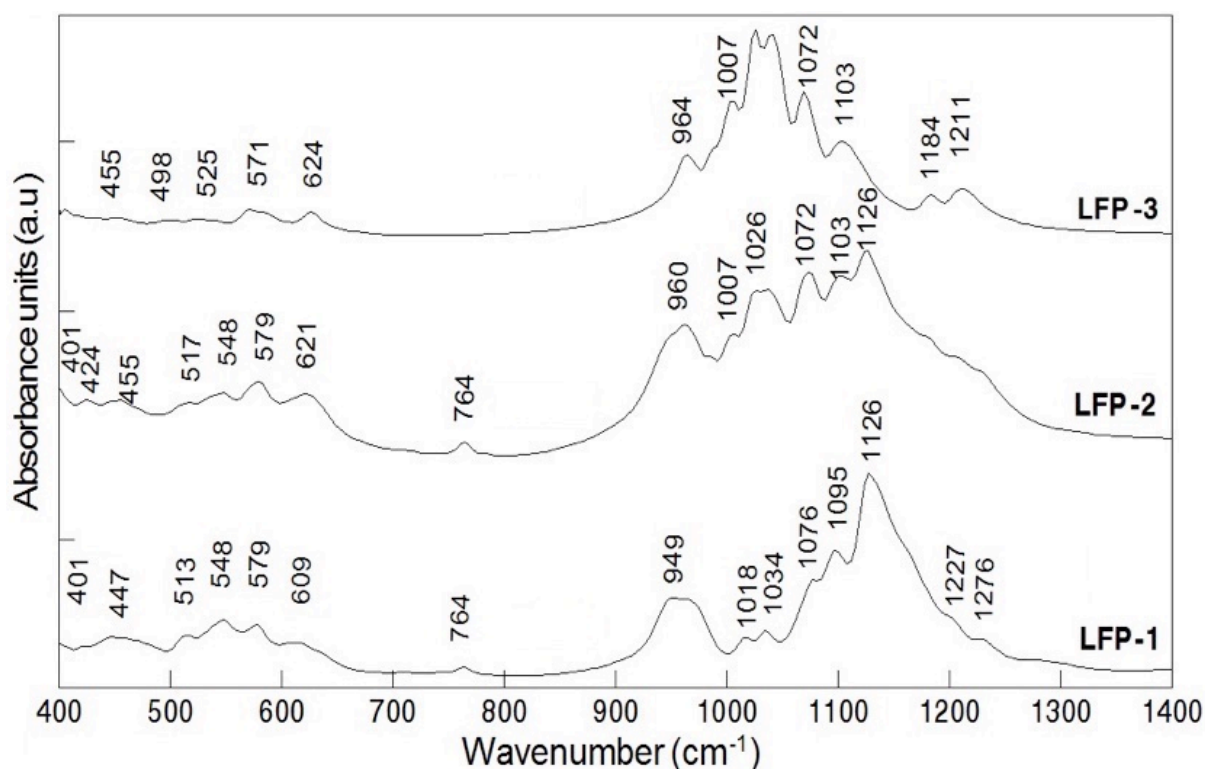


Figure 3. The FTIR spectra of LFP/C sample

The nasicon $\text{Li}_3\text{Fe}_2(\text{PO}_4)_3$ is built from anion framework of $\text{Fe}_2(\text{PO}_4)_3$ in which lithiums situated in the interstitial void in this framework [12]. The basic crystallography unit in diphosphate LiFeP_2O_7 is P_2O_7 anion with 2 main PO_4 tetrahedral bridging θ_{POP} angle. Modes in diphosphate consist of PO_3 and POP, and double bond PO [13]. The mode vibration located at 1227 cm^{-1} assigned to the terminal $\text{P}_2\text{O}_7^{4-}$ ions stretching mode [10] as presented in Figure 3. The spectra band appears at 764 cm^{-1} which is attributed to stretching modes of P-O-P bridges. The width and intense modes observed in 949 cm^{-1} are due to the normal vibration of the bridging oxygen atom with alkali ion [14]. Moreover, the asymmetric stretching vibration of PO_3 appears in 1126 cm^{-1} , with the highest intensity detected in LFP-1 and also found in LFP-2. The nasicon framework, $\text{Fe}_2(\text{PO}_4)_3$, consists of the octahedral of FeO_6 and tetrahedral of PO_4 ion. Meanwhile, the vibration octahedral of FeO_6 occurs below 450 cm^{-1} , and vibration of the valence bond from the PO_4^{3-} group is observed in between 400 and 700 cm^{-1} . The splitting of band peak at 1026 , 1038 , and 1072 cm^{-1} are attributed to the coupling vibration of PO_4 in the nasicon compound, and that is not observed in LFP-1. Conversely, these band peak are clearly observed in LFP-3 which is dominated by nasicon phase.

The more broadening bands observed in LFP-1 and LFP-2 show more variation of vibration occurring, and because of more phases is formed. In LFP-3 there is two phase, so the peak intensity can be differ clearly, even in the XRD pattern of LFP-3 show less peak with the high crystallinity.

CONCLUSION

In short, lithium iron phosphate/carbon composite-based material can be synthesized in three different temperature of calcination. Their phase and composition are also able to be determined. The diphosphate phase LiFeP_2O_7 is obtained at 400°C (LFP-1). The higher calcination temperature to at 600°C (LFP-3), decreased it gradually and transformed into nasicon $\text{Li}_3\text{Fe}_2(\text{PO}_4)_3$. The FTIR analysis also confirms the presence of their functional groups vibration modes. The highest composition of nasicon is produced in 85.72% after calcination at 600°C (LFP-3). It is also provide a low amount of impurity and give a stable LFP phase.

REFERENCES

- [1] Kasvayee, K.A., Synthesis of Li-ion battery cathode materials via freeze granulation, *Master's thesis*, Chalmers University of Technology, Sweden, 2011.
- [2] Satyavani, T.V.S.L., Kumar, A.S., and Rao, P.S., *Int. J. Eng. Sci. Technol.*, **2016**, 19(1), 178-188.
- [3] Chang, Z.R., Lv, H.J., Tang, H.W., Li, H.J., Yuan, X.Z., and Wang, H., *Electrochim. Acta*, **2009**, 54 (20), 4595-4599.
- [4] Zhang, B., Ou, X., Zheng, J.C., Ming, L., Han, Y.D., Wang, J.L. and Qin, S.E., *Electrochim. Acta*, **2014**, 133, 1-7.
- [5] Liu, X.H., and Zhao, Z.W., *Powder Technol.*, **2010**, 197(3), 309-313.
- [6] Wang, Y., Feng, Z.S., Chen, J.J., and Zhang, C., *Mater. Lett.*, **2012**, 71, 54-56.
- [7] Wang, J., Shao, Z. and Ru, H., *Ceram. Int.*, **2014**, 40 (5), 6979-6985.
- [8] Lu, C.Z., Fey, G.T.K., and Kao, H.M., *J. Power Sources*, **2009**, 189 (1), 155-162.
- [9] Wang, Y., He, Z.Y., Wang, Y.X., Fan, C., Peng, Q.L., Chen, J.J., and Feng, Z.S., *J. Colloid Interface Sci.*, **2018**, 512, 398-403.
- [10] Julien, C.M, Mauger, A., Zaghib, K. and Grout, H., *Inorganics*, 2014, 2(1), 132-154.

- [11] Hautier, G., Jain, A., Ong, S.P., Kang, B., Moore, C., Doe, R. and Ceder, G., *Chem. Matter*, 2011, 23(15), 3495-3508.
- [12] Andersson, A.S., Kalska, B., Eyob, P., Aernout, D., Häggström, L. and Thomas, J. O., *Solid State Ion*, **2001**, 140(1-2), 63–70.
- [13] Salah, A.A, Jozwiak, P., Zaghbi, K., Garbarczyk, J., Gendron, F., Mauger, A. and Julien, C.M., *Spectrochim. Acta. A*, **2006**, 65, 1007–1013.
- [14] Nasri, S., Megdiche, M. and Gargouri, M., *Ceram. Int.*, **2016**, 42 (1), 943-951.